DE LA RECHERCHE À L’INDUSTRIE

Thermal Hydraulic Analysis and Modelling of Tokamak Superconducting Magnets

26/06/2023

3rd year PhD Student: Quentin GORIT

INTRODUCTION

Superconductivity: Conductor capacity at **low temperature** to vanish **electrical resistance**

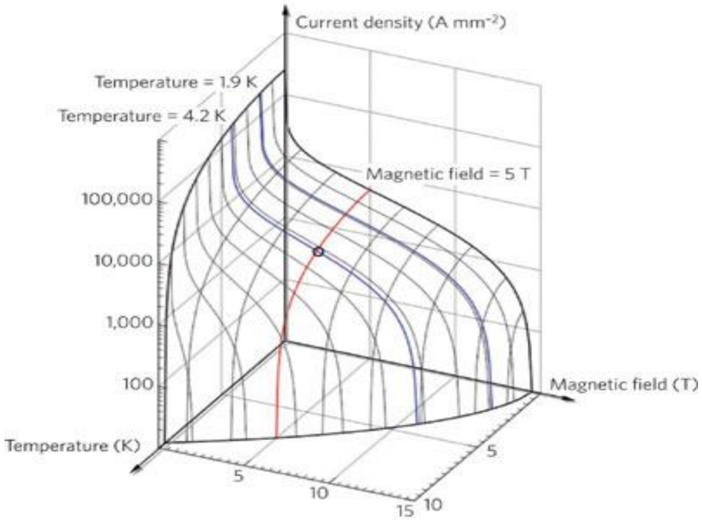

Magnet heat removal: Require **direct** or **indirect** cooling at **cryogenic temperatures**

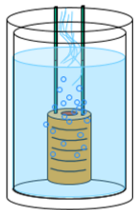

Direct cooling by bath

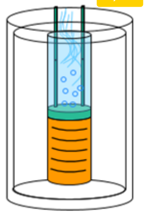

Indirect cooling by bath

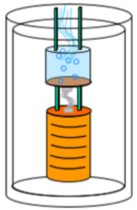

Indirect cooling by thermal link coupled with a bath

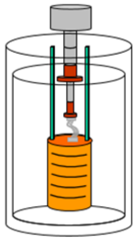

Indirect cooling by thermal link coupled with a cryocooler

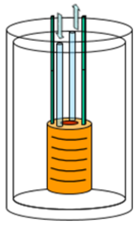

Direct cooling by internal forced flow

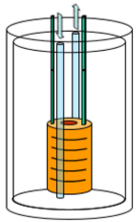

Indirect cooling by external forced flow

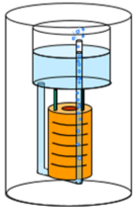

Indirect cooling by external two phase flow (thermosiphon)

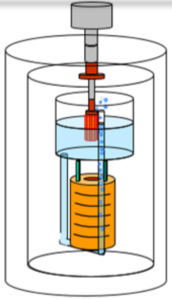

Indirect cooling by external two phase flow (thermosiphon) coupled with a cryocooler

SUMMARY

1- Direct internal forced flow cooled coil in tokamak

2- Indirect cooling by external two phase flow (thermosiphon) coupled with a cryocooler

3- Indirect cooling by thermal link (pulsating heat pipe) coupled with a cryocooler

1.1) Internal forced flow cooled coil in tokamak: Description

Forced flow cooled coil in tokamak:

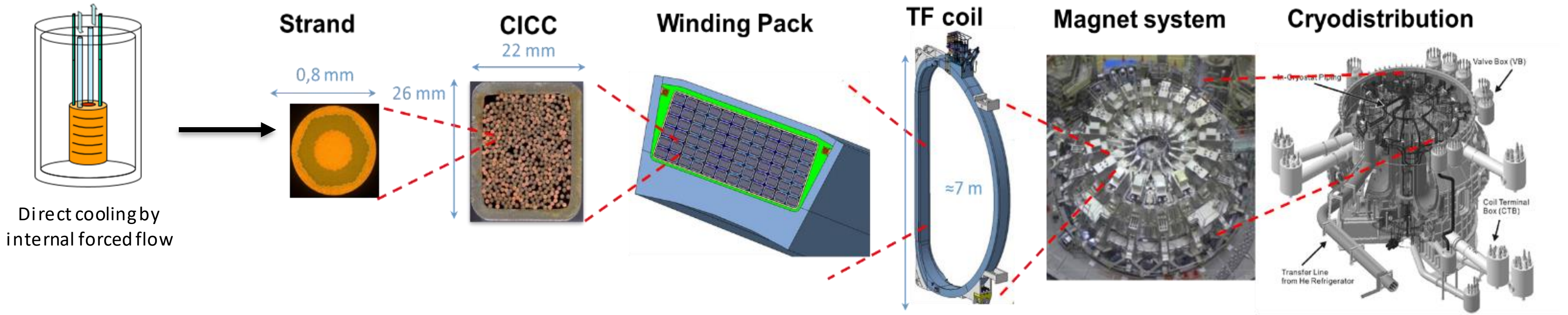

Direct cooling by internal forced flow

Operation: **Supercritical helium forced flow for heat removal** $(T_{He} \approx 4.5\ K, P_{He} \approx 5.5\ bar)$

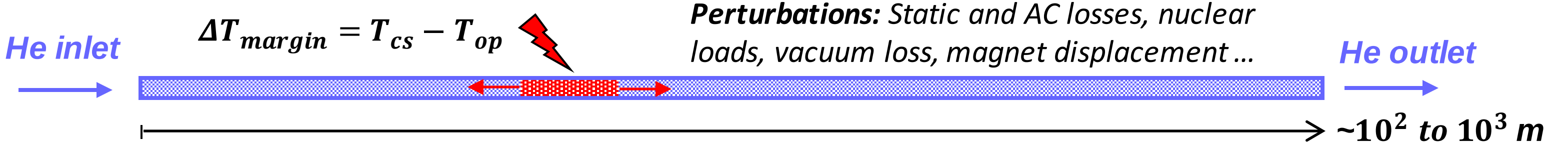

$$\Delta T_{margin} = T_{cs} - T_{op}$$

Perturbations: *Static and AC losses, nuclear loads, vacuum loss, magnet displacement …*

$\sim 10^2\ to\ 10^3\ m$

Quench: Irreversible **transition from superconducting to resistive state** starting from a **local perturbation**. The resistive **zone propagates** with **fluid flow and heat transfer mecanisms** and generates a large power by **Joule effect**.

If not quickly detected, **possible permanent damage** of the magnet

1.2) Internal forced flow cooled coil in tokamak: Context

Problematic: **How to confirm the safe operation of tokamak superconducting magnets ?**

***Context*:** Commissioning of **JT-60SA** magnets & Preparation of **DEMO/ ITER** operation

Project: Study **heat transfers** and **helium flows** present in magnets for **operational domain definition** and **quench protection** purposes

1- Thermal hydraulic properties characterization of cable-in-conduit conductor

2- Study of the magnet behavior during quench propagation phenomena

3- Development of tools at reduced computation time useful to prepare the operation

1.3) Internal forced flow cooled coil in tokamak:
1-D thermal hydraulic model of CICC

Energy balance for conductor and conduit wall (solids, i=s or j):

Geometrical parameters unknown

$$\rho_i\, C_i \frac{dT_i}{dt} = \frac{d}{dx}\left(k_i \frac{dT_i}{dx}\right) + \boldsymbol{h}\frac{\boldsymbol{P_{w,i}}}{\boldsymbol{A_i}}(T - T_i) + q_{Joule,i} + q_{ext,i}$$

Heat transfers parameters unknown

Mass, momentum and energy balances for helium flow (fluids):

$$\frac{d\rho}{dt} + \frac{d\rho v}{dx} = 0$$

Flow parameters unknown

$$\frac{d\rho v}{dt} + \frac{d\rho v^2}{dx} = -\frac{dp}{dx} - \frac{\boldsymbol{f}\rho v|v|}{2\boldsymbol{D_h}}$$

$$\rho C_v\left(\frac{dT}{dt} + v\frac{dT}{dx}\right) + \rho\phi C_v T\frac{dv}{dx} = \frac{d}{dx}\left(k\frac{dT}{dx}\right) + \boldsymbol{h}\frac{\boldsymbol{P_{w,s}}}{\boldsymbol{A}}(T_s - T) + \boldsymbol{h}\frac{\boldsymbol{P_{w,j}}}{\boldsymbol{A}}(T_j - T) + \frac{\boldsymbol{f}\rho v^2|v|}{2D_h}$$

Possibility of quasy 3-D model of the magnet → 1-D CICC models + 2-D casing cross-sections models

1.4) Internal forced flow cooled coil in tokamak: Thermal hydraulic properties characterization of cable-in-conduit conductor

Geometrical properties of CICC from X-ray tomography

Strands trajectories from X-ray tomography

(Data courtesy of INFLPR)

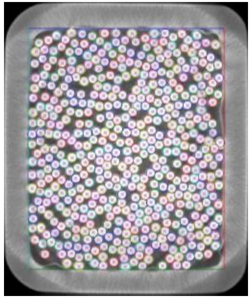

CICC of JT-60SA toroidal field coil

Local properties

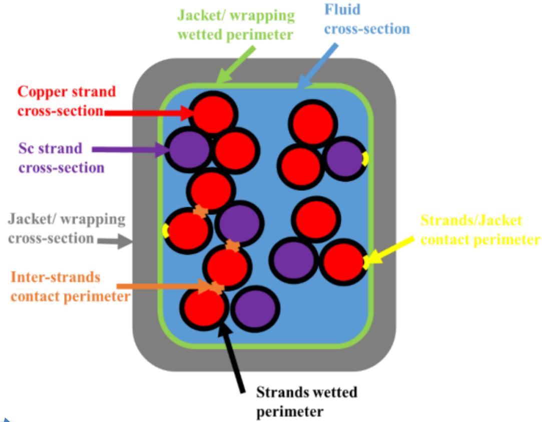

3-D reconstruction for CFD simulations

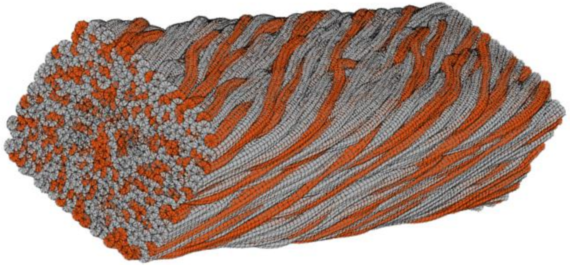

Effective properties

Wetted perimeters: $P_{w,s}$, $P_{w,j}$

- ❖ Distances between strands centers
- ❖ Jacket locations
- ❖ Interpenetration lengths

Fluid surface: A

- ❖ Strands lengths
- ❖ Solids' volumes
- ❖ Porosity

Hydraulic diameter: $D_h = 4\frac{A}{P_{w,s}+P_{w,j}}$

Input geometrical parameters in models

1.4) Internal forced flow cooled coil in tokamak: Thermal hydraulic properties characterization of cable-in-conduit conductor

OTHELLO facility for stationary and transient forced-flow experiments

❖ **Nitrogen gas** at **equivalent conditions to supercritical helium** forced flow regarding thermal conductivity, Reynolds and Prandtl numbers:

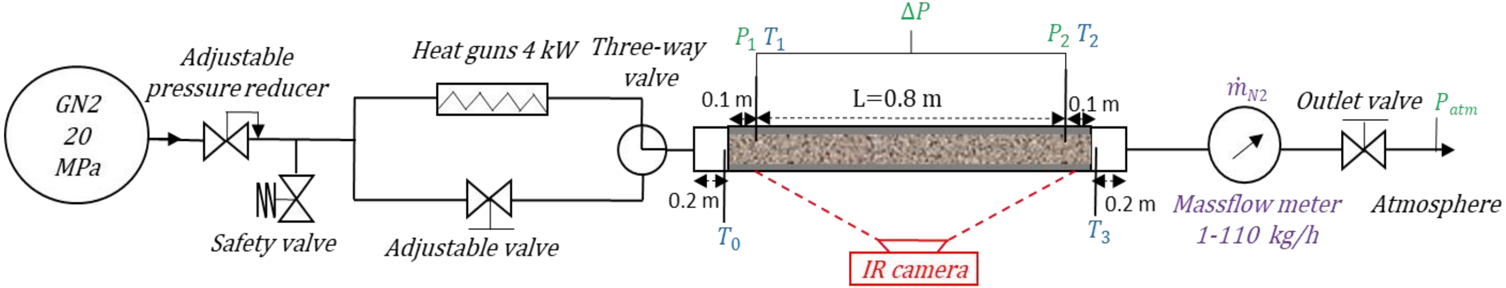

Stationnary experiments

❖ ***Pressure drop measurements on straight/ bended sample*** :

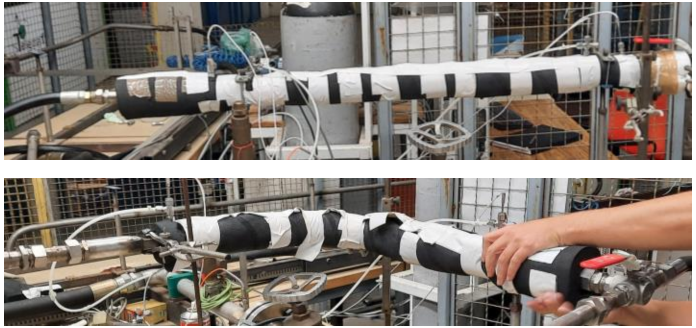

Transient experiments

❖ ***Heat pulse measurements on straight sample with infrared camera*** :

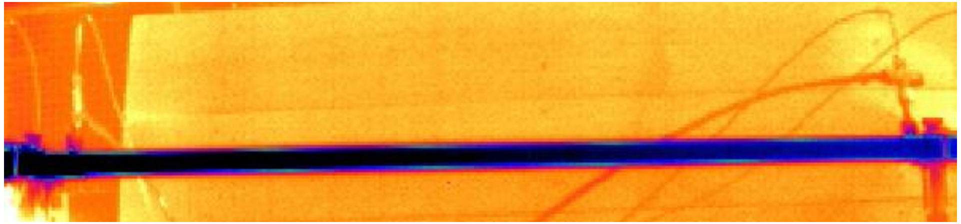

(Study in collaboration with IUSTI, J. Gaspar)

1.4) Internal forced flow cooled coil in tokamak: Thermal hydraulic properties characterization of cable-in-conduit conductor

Flow parameters from stationnary experiments

❖ **Darcy-Forchheimer equation:** $\rho \frac{dp}{dx} = -(\frac{\mu}{\boldsymbol{K}}\eta + \boldsymbol{\beta}\eta^2)$

(Momentum balance for flow in porous media)

→

❖ **Analogy to Darcy-Weisbach equation:** $f = \frac{2D_h^2\Phi}{\boldsymbol{K}}\frac{1}{Re} + 2D_h\Phi^2\boldsymbol{\beta})$

(Momentum balance for flow in smooth tube)

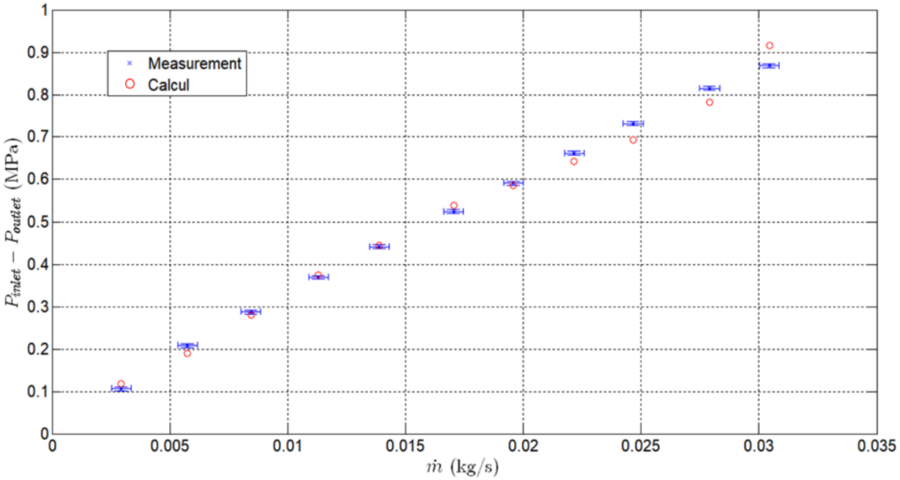

Pressure drop VS mass flow

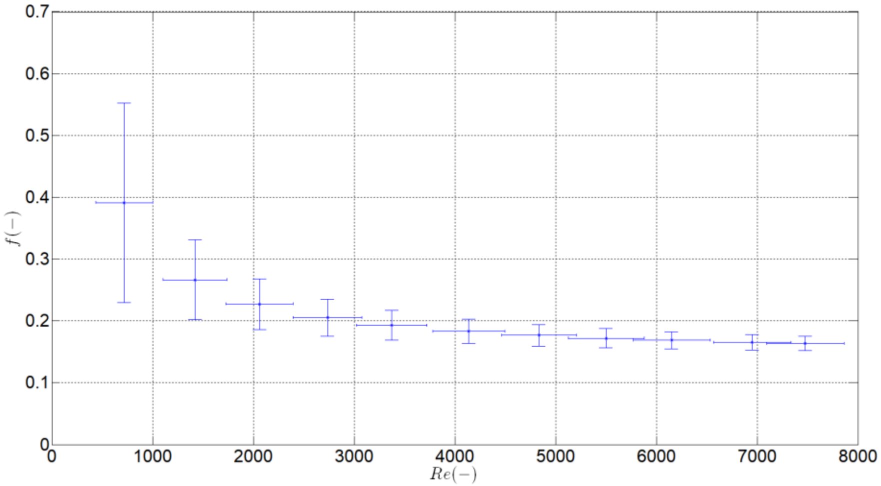

Friction factor VS Reynolds number

Permeability $\boldsymbol{K}$ and Inertia coefficent $\boldsymbol{\beta}$ estimation

Friction factor $\boldsymbol{f}$ estimation for pressure profile modelling

1.4) Internal forced flow cooled coil in tokamak: Thermal hydraulic properties characterization of cable-in-conduit conductor

Convective heat transfer coefficient from transient experiments:

❖ **Heat pulse** from fluid **inlet** temperature

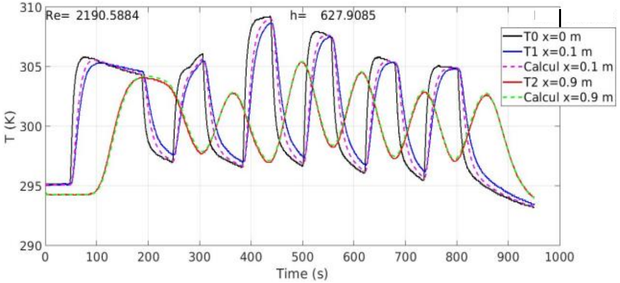

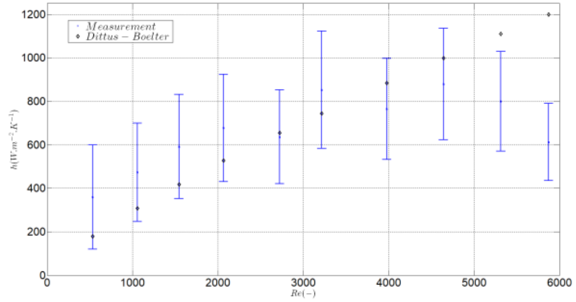

❖ **3 temperatures model: 1-D equivalent** and **fictive porous media** (Nitrogen, strands, jacket)

Solids energy balances:

$$\rho_s C_s \frac{dT_s}{dt} = k_s \frac{d^2 T_s}{dx^2} + \boldsymbol{h} \frac{\boldsymbol{P_{w,s}}}{\boldsymbol{A_s}} (T - T_s)$$

$$\rho_j C_j \frac{dT_j}{dt} = k_j \frac{d^2 T_j}{dx^2} + \boldsymbol{h} \frac{\boldsymbol{P_{w,j}}}{\boldsymbol{A_j}} (T - T_j)$$

Fluid mass, momentum, energy balances:

$$\frac{d\rho v}{dx} = 0$$

$$\frac{dp}{dx} = -\frac{\boldsymbol{f}\, \rho\, v^2}{2\, \boldsymbol{D_h}}$$

$$\rho C \frac{dT}{dt} + \rho C v \left(\frac{dT}{dx} - \mu_{JT} \frac{dp}{dx}\right) = \boldsymbol{h} \frac{\boldsymbol{P_{w,s}}}{\boldsymbol{A}} (T_s - T) + \boldsymbol{h} \frac{\boldsymbol{P_{w,j}}}{\boldsymbol{A}} (T_j - T)$$

Numerical solutions:

Semi-analytical using Fourier transform (conductionless solids and no compressibillity effects)

Numerical using implicit volumes finite method

Inverse procedure: Estimation of ***h*** solutions with a **least square method**

$$\begin{matrix} T_{Exp,inlet} \\ h_{guess} \end{matrix} \rightarrow \boxed{\text{3 Temperatures model}} \rightarrow S = \left(T_{Calc,outlet} - T_{Exp,outlet}\right)^2 \rightarrow \min(S)$$

Convective heat transfer coefficient *h*

Input convective heat transfer coefficient for temperature profile modelling

1.5) Internal forced flow cooled coil in tokamak: Study of the magnet behavior during quench propagation phenomena

Quench tests of JT-60SA TFC in Cold Test Facility:

- 18 TF coils and **2 spares tested:**

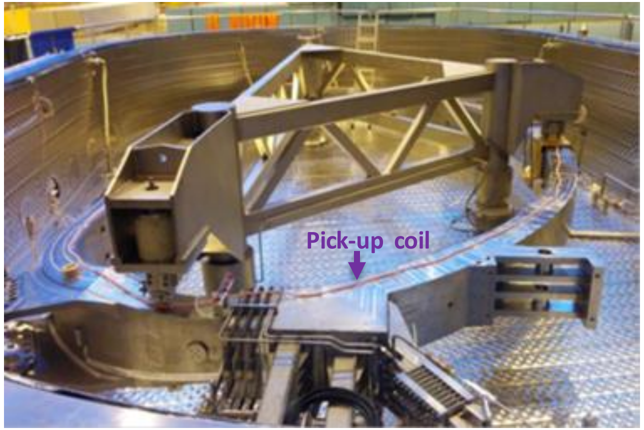

- **Several quench conditions tested on spare coil:**

TFC02 Tests	I (kA)	B_{max} (T)	$T_{cs,min}$ (K)	τ_h (s)
Acceptance	25.7	3.05	7.42	0.1
Delayed detection	25.7	3.05	7.42	0.5
75 % I_{nom}	19.5	2.29	7.83	0.1
50 % I_{nom}	12.9	1.52	8.24	0.1

(Study in Collaboration with IRFU, R. Vallcorba)

Quench propagation measurements:

- **Pressure, mass flow and temperature** measurements **at magnet inlet** and **outlet**

- **Voltage** measurements on **CICC** and a **pick-up coil**:

Quench detection → Fast current discharge → magnetic fields variations → **inductive voltage**

$$\gamma_{DP} = \left(\frac{V_{b,DP}}{V_{pickup}}\right)_{PFCD} = \left(\frac{V_{DP,inductive}}{V_{pickup}}\right)_{quench}$$

$$\underbrace{V_{b,DP} = L_{DP}\frac{dI}{dt} + M_{DP}\frac{dI_p}{dt}}_{V_{DP,inductive}} + \underbrace{R_{DP}I}_{V_{DP,resistive}}$$

1.5) Internal forced flow cooled coil in tokamak:
Study of the magnet behavior during quench propagation phenomena

1-D SuperMagnet model:

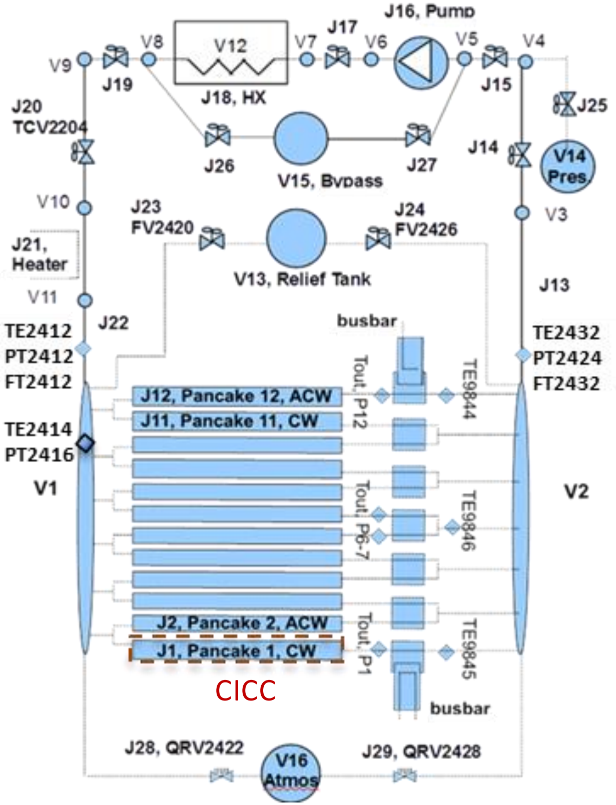

Numerical and experimental results:

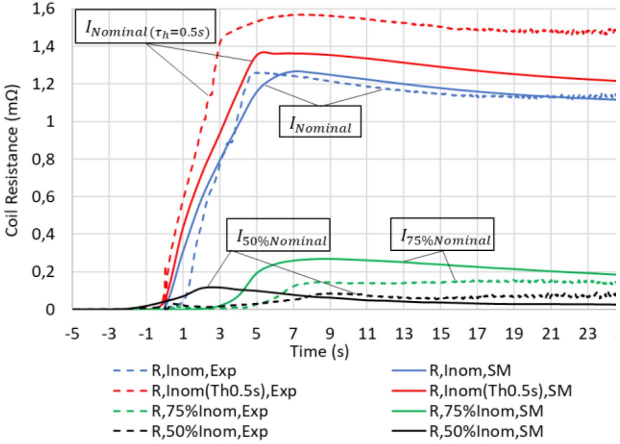

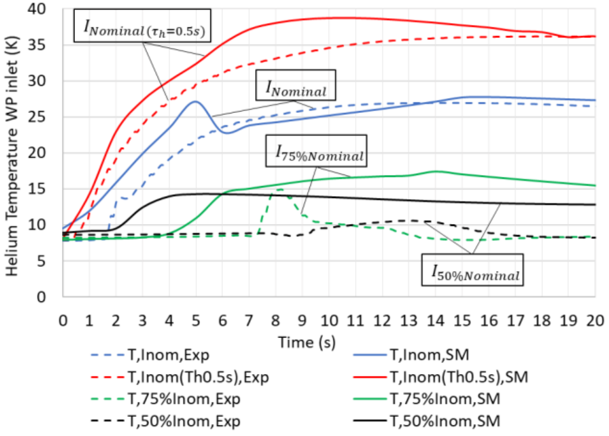

❖ Exp/Simu **consistent results** (with difficulties to simulate reduced current tests)

❖ **Reduced current impact**:
Low **quench propagation velocity** increasing the **propapagation time before detection**

❖ **Delayed detection impact**:
Increase of joule energy dissipated before and during current discharge increasing **hotspot temperature**

1.5) Internal forced flow cooled coil in tokamak: Study of the magnet behavior during quench propagation phenomena

Extrapolation from testing to tokamak conditions

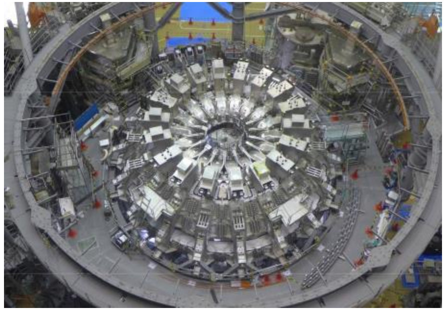

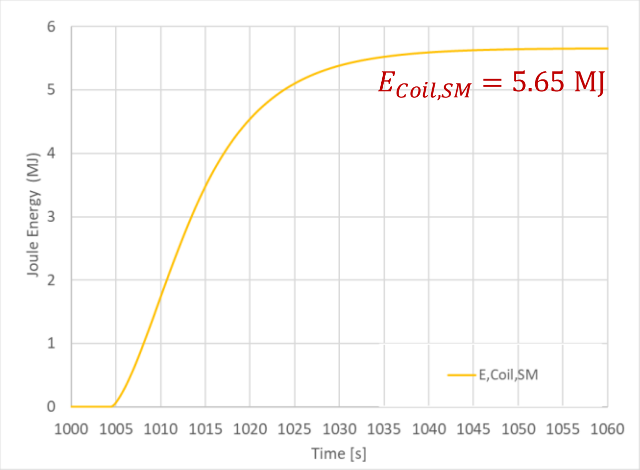

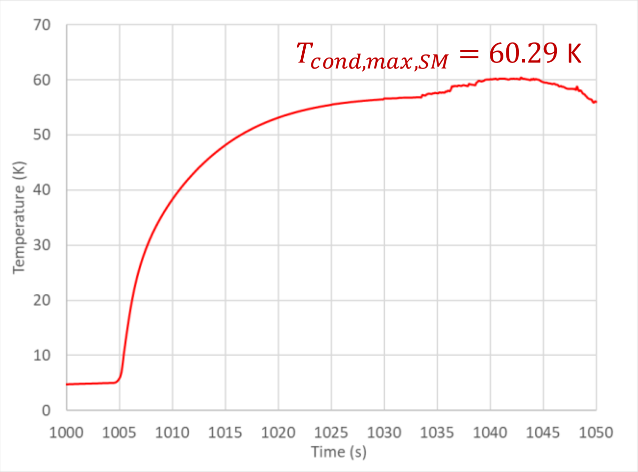

Heat loads on JT-60SA cryogenic plant:

+ 5.65 MJ Conservative joule energy dissipated during the **quench of one TFC** (10 % of the TF stored magnetic energy)

+ 11 MJ Joule energy dissipated in the **18 TFC thick casings by eddy currents** because of the Fast Current Discharge

(M. Wanner, "JT -60SA Plant Integration Document (PID)," V4.2)

Quench maximal conductor temperature criteria:

$T_{cond,\,maximal} =$ **60.29 K< 150 K** (criteria for non-adiabatic conductor)

Quench criticality: $v_{q,P1,SM} = \mathbf{19.5\ m/s} \rightarrow E_{P1,SM} = 0.585\ \mathrm{MJ} \rightarrow \boldsymbol{T_{cond,P1(inlet),SM} = 60.29\ K}$ *(Study in collaboration with F4E, A. Louzguiti)*

1.6) Internal forced flow cooled coil in tokamak:
Development of tools at reduced computation time

Modelling problematic: **Numerical difficulties** requiring **large computational ressources**

Objective: Fast assessment of **operational windows** and **magnet safety**

Application: **Design** and **real time control** tools

Simplified and tailored models

1-D **operation** simplified model

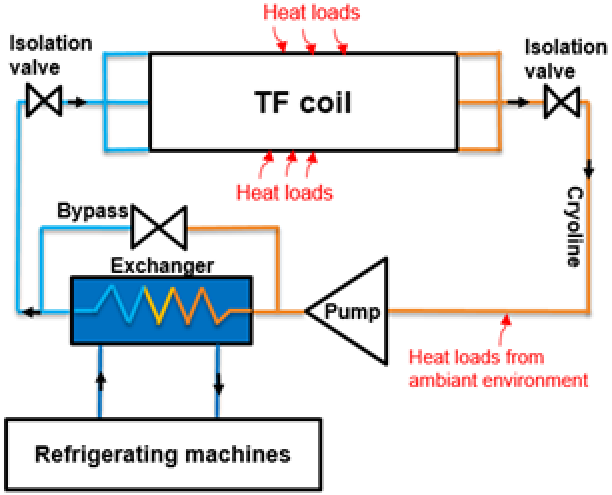

1-D **quench** simplified model

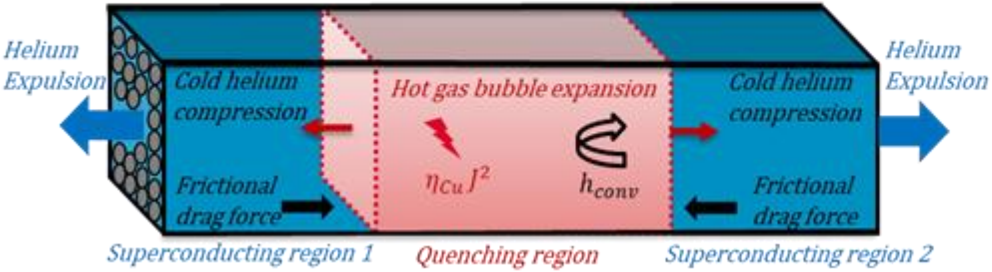

2.1) Indirect cooling by external two phase flow coupled with a cryocooler: Principles

Advantage:

Natural circulation avoiding high pumping cost

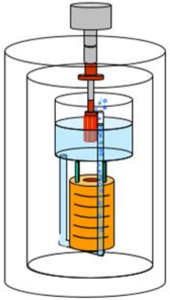

Indirect cooling by external two phase flow (thermosiphon) coupled with a cryocooler

Thermosiphon:

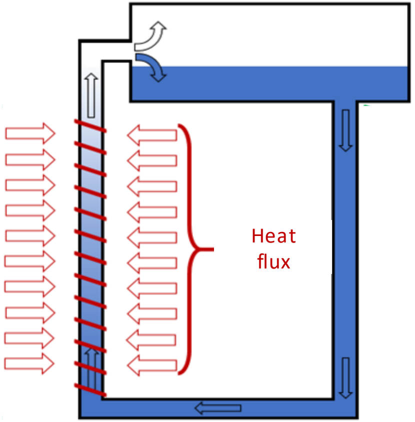

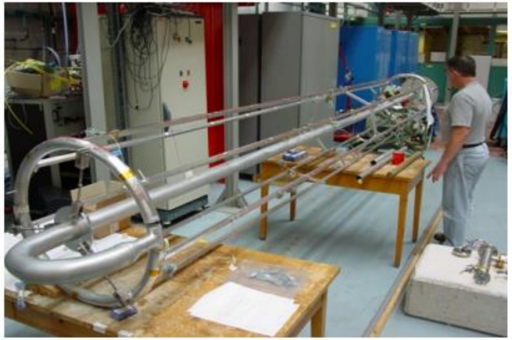

Thermosiphon loop for CMS particle detector of LHC at CERN (Swiss)

Cryocooler:

Succesive compression and expansion of helium decreasing the cold head temperature

Cold head reaching T < 4 K

2.2) Indirect cooling by external two phase flow coupled with a cryocooler: Experimental characterization of a thermosiphon loop

Monitor **convective heat transfer** between **tube** and **helium two-phase flow** in stationnary state

Heat transfer coefficient estimation using measurements and a 1-D vertical model of **helium two phase flow**

ThermAutonome facility at CEA Saclay (France)

$(T_{He} \approx 4.5\ K, P_{He} \approx 1.3\ bar)$

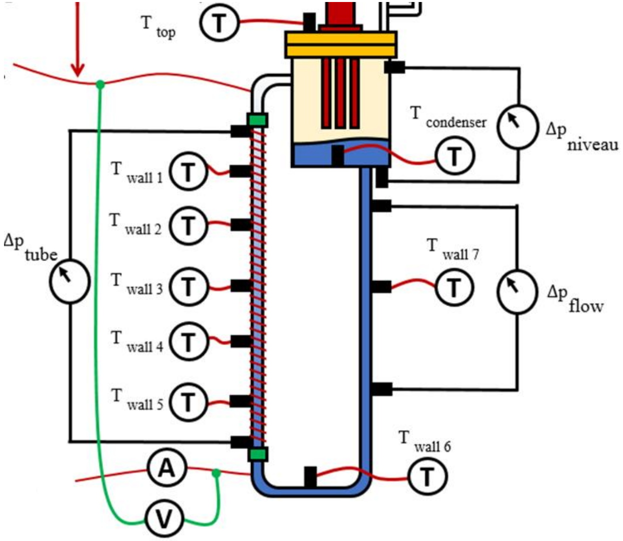

Two phase flow (left tube)

Single phase flow (right tube)

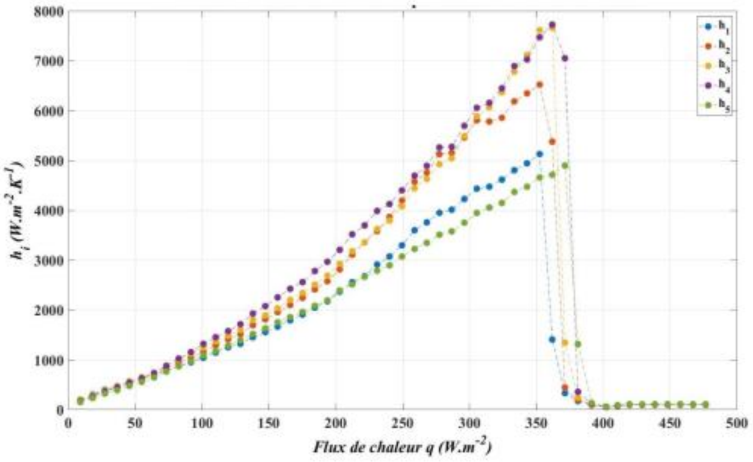

Observation of intense convective heat transfers during boiling follow by a decrease after vapor film establishment drying out the tube wall

3.1) Indirect cooling by thermal link coupled with a cryocooler: Different thermal links

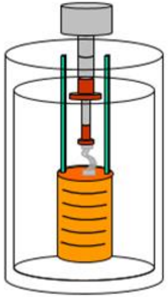

Indirect cooling by thermal link coupled with a cryocooler

Conventional Copper block

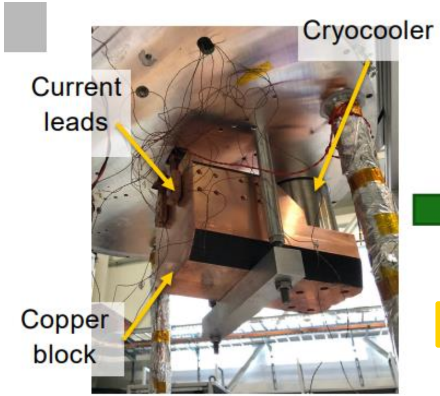

Test 2 kA current leads

Cryogenic pulsating heat pipe (helium, nitrogen, neon or hydrogen)

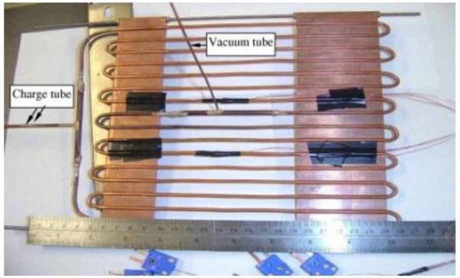

Nitrogen PHP in Laboratory
(Jiao et al., https://doi.org/10.1016/j.ijheatmasstransfer.2009.03.013.)

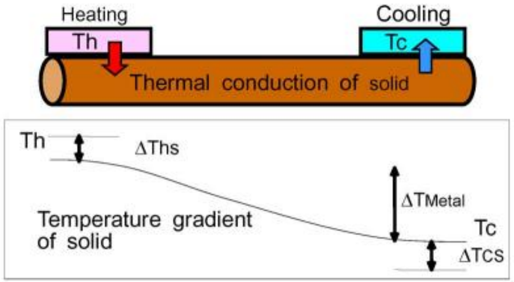

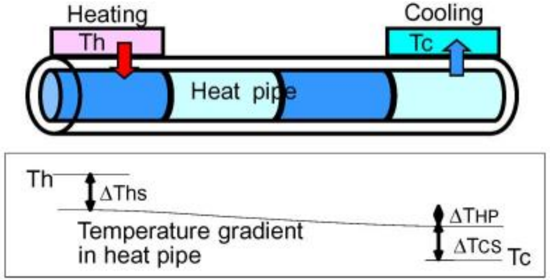

(Mito, Toshiyuki, et al., https/doi.org/10.1109/TASC.2010.2100356)

Advantages of pulsating heat pipe:

- ❖ Lower weight
- ❖ higher thermal performance (effective thermal conductivity increased of factor 40 to 100 using N2)

3.2) Indirect cooling by thermal link coupled with a cryocooler: Pulsating heat pipe

Principle:

Train of alternating liquid slug and vapor bubbles surrounded by liquid film

↓

Expansion and compression of vapor bubbles induce flow oscillations

↓

Liquid transfers heat from hot to cold par

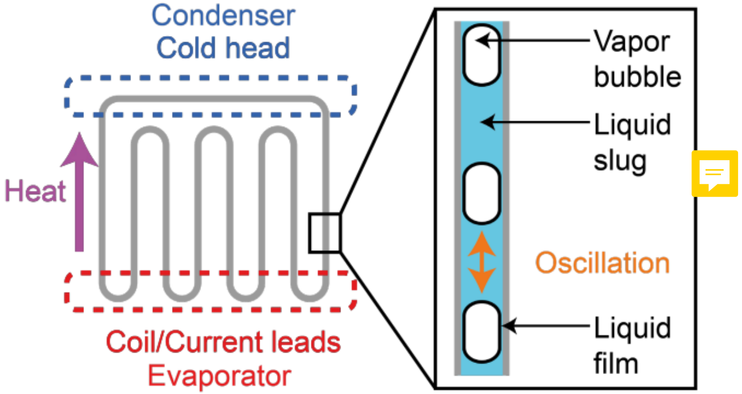

Limitation:

Dry out phenomena can arise stopping oscillation and heat transfe (no liquid film anymore) after reaching a heat load treshold

Applications:

- ❖ HTS magnets (even in rotation since PHP can work without gravity) and current leads
- ❖ Thermal shield for LTS magnet
- ❖ Portable cooling system for HTS coil antenna
- ❖ Sc. accelerator cavities
- ❖ Sc. electronics applications
- ❖ Quantum computing

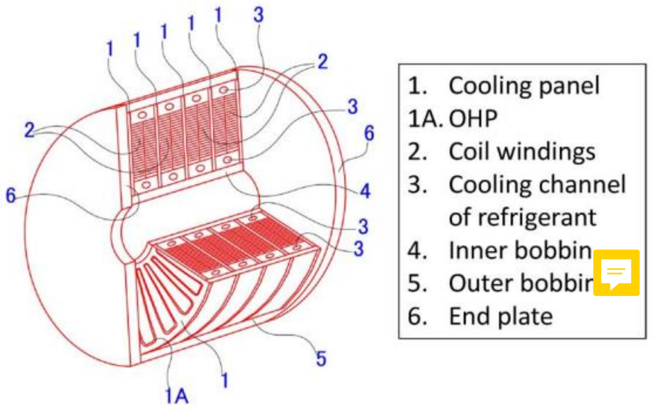

Conceptual design of OHPs imbedded in a HTS magnet

(Mito, Toshiyuki, et al., https/doi.org/10.1109/TASC.2010.2100356)

3.3) Indirect cooling by thermal link coupled with a cryocooler: Existing facilities for pulsating heat pipe testing

Large facility at CEA Saclay (France)

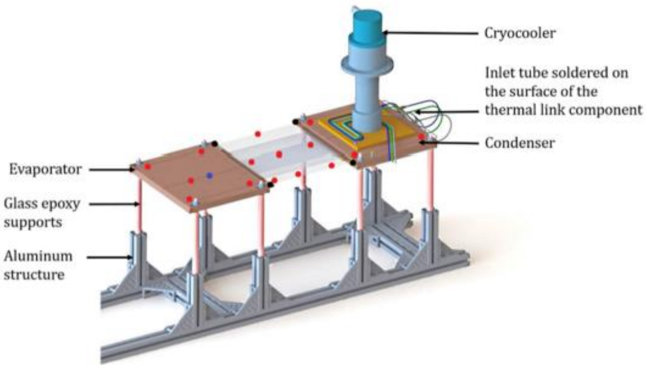

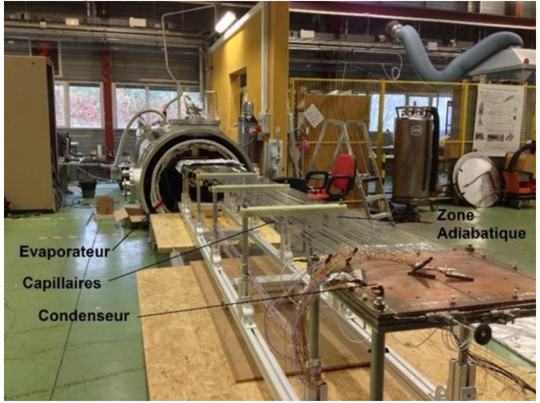

(Romain Bruce et al., https/doi/10.1109/TASC.2019.2902978)

Adaptable facility at NIFS (Japan)

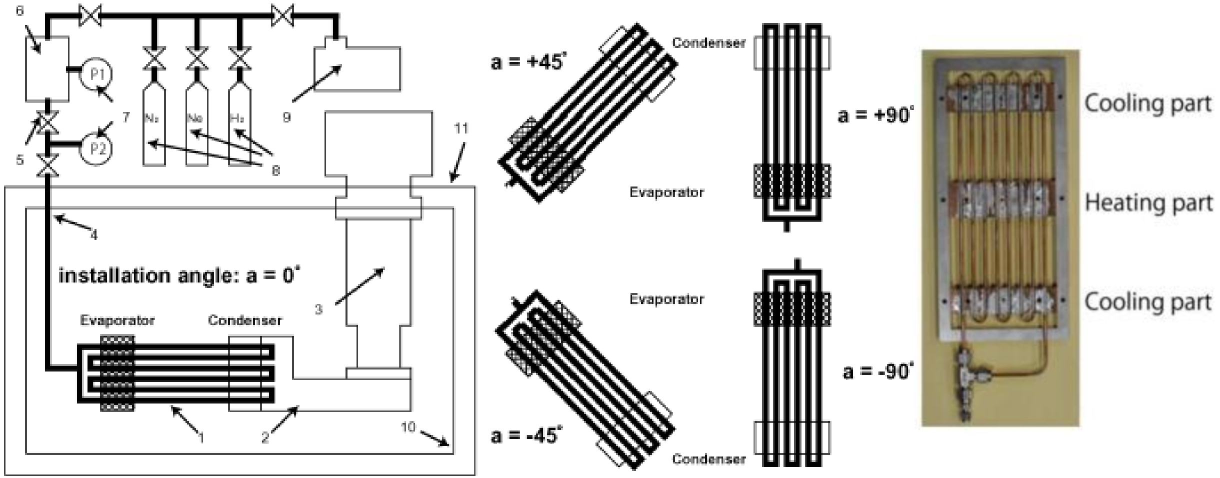

(Mito, Toshiyuki, et al., https/doi.org/10.1109/TASC.2010.2100356)

Effective thermal conductivity estimation:

$$k = \frac{\text{heat input}}{\text{temperature difference}} \times \frac{\text{distance}}{\text{cross} - \text{sectional area}}$$

Possible studies on:

- ❖ Working fluids ($T_{He} \approx 4\ K, T_{Ne} \approx 30\ K, T_{N2} \approx 80\ K$)
- ❖ Orientations (vertical, horizontal …)
- ❖ Dimensions (tube diameter, size …)
- ❖ Heating/cooling locations (center/extremities)

Conclusion

1- Direct internal forced flow cooling

Heat removal of LTS magnets for tokamak insured by high convective heat transfers

Reliable simulations and magnet safety assessments after thermal hydraulic properties and quench behavior characterization

2- Indirect cooling by external two phase flow (thermosiphon) coupled with a cryocooler

Passive device saving pumping cost

Insure high convection for heat removal in boiling regime

3- Indirect cooling by thermal link (pulsating heat pipe) coupled with a cryocooler

Low weight and high thermal performance

Passive device (no pumping nor gravity required)

Potential cutting-edge technology for HTS magnets cooling

Possible characterization of the optimal configurations

Thank you for your attention

Questions ?

Flow model for friction factor analysis

Assuming **compressible, isothermal and ideal fluid** in order to model **the regular pressure drop**:

$$\left.\begin{aligned} &\frac{d(\rho(x)v(x))}{dx} = 0 \\ &\frac{dT(x)}{dx} = 0 \\ &\rho(x) = \frac{p(x)}{R'T} \\ &\eta = \frac{\dot{m}}{A\,\phi} \end{aligned}\right\}$$

Darcy-Weisbach equation:

$$\frac{dp(x)}{dx} = -\frac{f\,\rho(x)\,v(x)^2}{2\,D_h}$$

Darcy-Forchheimer equation:

$$\boxed{\rho(x)\frac{dp(x)}{dx} = -(\frac{\mu}{K}\eta + \beta\eta^2)}$$

Darcy-Forchheimer and Darcy-Weisbach analogy:

$$\boxed{f = 2D_h(\frac{D_h}{K}\frac{1}{Re} + \beta)}$$

$$\int_0^L dx$$

$$\boxed{-(\frac{1}{2R'T})\frac{p_{out}^2 - p_{in}^2}{L\,\mu\,\eta} = (\frac{1}{K} + \beta\frac{\eta}{\mu})}$$

Analogy to **porous media**: **Permeability** **Inertial coefficient**

Linear regression on experimental results for flow parameters deduction

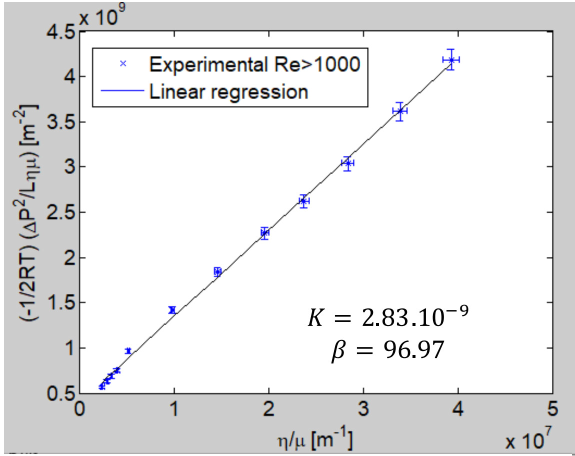

$K = 2.83.10^{-9}$

$\beta = 96.97$

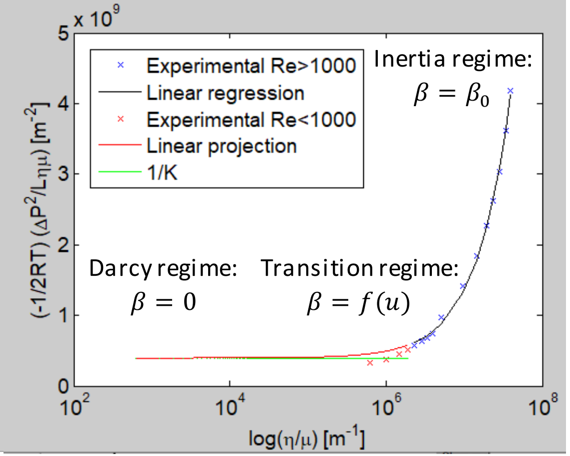

Inertia regime: $\beta = \beta_0$

Darcy regime: $\beta = 0$

Transition regime: $\beta = f(u)$

M3T : Finite volumes numerical method

Governing equations: $\frac{d(\rho\, v)}{dx} = 0 \qquad \frac{dp}{dx} = \frac{f\,\rho v^2}{2\, D_h}$

Fluid: $\rho C_p \frac{dT}{dt} + \rho C_p v \frac{dT}{dx} = \frac{d}{dx}\left(k\frac{dT}{dx}\right) + S_{JT} + h\frac{P_{w,s}}{A}(T_s - T) + h\frac{P_{w,j}}{A}(T_j - T)$

Solids: $\rho_s C_s \frac{dT_s}{dt} = \frac{d}{dx}\left(k_s \frac{dT_s}{dx}\right) + h\frac{P_{w,s}}{A_s}(T - T_s) \qquad \rho_j C_j \frac{dT_j}{dt} = \frac{d}{dx}\left(k_j \frac{dT_j}{dx}\right) + h\frac{P_{w,j}}{A_j}(T - T_j)$

Boundary conditions at inlet and outlet (6 eqs):

Fluid: $\rho C_p \frac{dT}{dt} + \rho C_p v \frac{dT}{dx} = \frac{d}{dx}\left(k\frac{dT}{dx}\right) + S_{JT} + h\frac{P_{w,s}}{A}(T_s - T) + h\frac{P_{w,j}}{A}(T_j - T)$

Solids: $\rho_s C_s \frac{dT_s}{dt} = \frac{d}{dx}\left(k_s \frac{dT_s}{dx}\right) - h_{ext}(T_s - T_{ext}) + h\frac{P_{w,s}}{A_s}(T - T_s) \qquad \rho_j C_j \frac{dT_j}{dt} = \frac{d}{dx}\left(k_j \frac{dT_j}{dx}\right) - h_{ext}(T_j - T_{ext}) + h\frac{P_{w,j}}{A_j}(T - T_j)$

Initial conditions: $T = T_s = T_j = T_{steadystate}$

$$\underbrace{\int_{t_0}^{t_1}\int_{i-1}^{i+1} dx\, dt}$$

Integrated form:

Fluid:

$$a_i T_i = a_{i+1} T_{i+1} + a_{i-1} T_{i-1} + a_{i,hs} T_{s,i} + a_{i,hj} T_{j,i} + b_i$$

Strands:

$$a_i T_{s_i} = a_{i+1} T_{s_{i+1}} + a_{i-1} T_{s_{i-1}} + a_{i,hs} T_i + b_i$$

Jacket:

$$a_i T_{j_i} = a_{i+1} T_{j_{i+1}} + a_{i-1} T_{j_{i-1}} + a_{i,hj} T_i + b_i$$

Inversion:

$$A\,T = B$$

SuperMagnet: CICC thermal hydraulic model

Energy balance for heat conduction model in conductor and conduit wall:

$$A_i\ \rho_i\ C_i\frac{dT_i}{dt} - \frac{d}{dx}(A_i\ k_i\frac{dT_i}{dx}) = \sum_{j=1,j\neq i}^{N}\frac{(T_j - T_i)}{R_{th,ij}} + \sum_{h=1}^{H} h_{i,h}\ P_{i,h}(T_h - T_i) + q_{Joule,i} + q_i$$

Mass, momentum and energy balances for flow model:

$$\rho_h\frac{d(A_h v_h)}{dt} + \rho_h v_h\ \frac{d(A_h v_h)}{dx} + A_h\frac{dp_h}{dx} - \rho_h v_h^2\frac{dA_h}{dx} = -A_h F_h - \sum_{k=1,k\neq h}^{H}(\Gamma_{hk}^{v} - \Gamma_{hk}^{\rho})$$

$$A_h\frac{dp_h}{dt} + A_h v_h\ \frac{dp_h}{dx} + \rho_h c_h^2\frac{d(A_h v_h)}{dx} - \rho_h v_h^2\frac{dA_h}{dx} = \phi_h A_h v_h F_h + \phi_h q_h + \phi_h q_{cf,h} - \sum_{k=1,k\neq h}^{H}(c_h^2\Gamma_{hk}^{\rho} + \phi_h[\Gamma_{hk}^{e} - v_h\Gamma_{hk}^{v} - (h_h - \frac{v_h^2}{2})\Gamma_{hk}^{\rho}])$$

$$A_h\rho_h C_h\left(\frac{dT_h}{dt} + v_h\frac{dT_h}{dx}\right) + \rho_h\ \phi_h\ C_h\ T_h\ \frac{dv_h}{dx} = A_h v_h F_h + q_h + q_{cf,h} - \sum_{k=1,k\neq h}^{H}(\Gamma_{hk}^{e} + v_h\Gamma_{hk}^{v} - (h_h - \frac{v_h^2}{2} - \phi_h T_h C_h)\Gamma_{hk}^{\rho})$$

CiccStream CICC thermal hydraulic model

Quenching region :

Model at 2 temperatures:

Mass balance completed by state equation (ideal gas law) for flow model:

$$\rho_q = \frac{\rho_0 L_q}{\sum_{i=1}^{2} X_{q,i}} \qquad p_q = \rho_q R_{gas} T_q \qquad v_q = \frac{x}{\sum_{i=1}^{2} X_{q,i}} \sum_{i=1}^{2} \frac{dX_{q,i}}{dt}$$

Energy balance for conductor/helium:

$$(A_{Cu}\, \rho_{Cu}\, C_{Cu} + A_{NbTi}\, \rho_{NbTi}\, C_{NbTi} + A_h\, \rho_q\, C_h)\frac{dT_q}{dt} = h_{conv}\, P_{w,j}\left(T_j - T_q\right) + \frac{\eta_{Cu} I^2}{A_{Cu}}$$

Energy balance for conduit wall:

$$A_j\, \rho_j\, C_j \frac{dT_j}{dt} = h_{conv}\, P_{w,j}(T_q - T_j)$$

Superconducting region :

Model at 1 temperature: T_h

Mass and momentum balances completed by state equation for flow model:

$$\frac{d\rho_h}{dt} + \frac{d(\rho_h v_h)}{dx} = 0$$

$$\frac{dp_h}{dx} = -\frac{f \rho_h v_h |v_h|}{2D_h}$$

$$\rho_h C_h \frac{dT_h}{dt} = T_h C_\beta \frac{d\rho_h}{dt}$$

Quench front matching conditions

Equal velocities between $x = X_q^-$ and $x = X_q^+$:

$$\frac{dX_q}{dt} = v_q\Big|_{x=X_q^-} = v_h\Big|_{x=X_q^+} = \left(\frac{2\, D_h}{f}\right)^{\frac{1}{2}} \left(\frac{-{c_h}^2}{\rho_h}\frac{d\rho_h}{dx}\right)^{\frac{1}{2}}\Bigg|_{x=X_q^+}$$

Equal pressures between $x = X_q^-$ and $x = X_q^+$:

$$p_q\Big|_{x=X_q^-} = p(\rho_h, S_0)\Big|_{x=X_q^+}$$

Stream CICC thermal hydraulic model

Superconducting and quenching volumes:

$$\frac{dW(t)}{dt} = -p_{He}(t)\frac{dV_{cold}(t)}{dt} = p_{He}(t)\frac{dV_{hot}(t)}{dt}$$

Normal length propagation:

$$v_q(t) = 0.766\left(\frac{2\,D_h}{f_{CICC}}\right)^{\frac{1}{5}}\left(\frac{r\,L_{q,ini}\,\alpha_0 J_0^2}{c_0}\right)^{\frac{2}{5}}\frac{1}{t^{\frac{1}{5}}}$$

$$L_q(t) = 2\,\left(v_q(t)\;t + \frac{L_{q,ini}}{2}\right)$$

Stream 0-D

- ❖ CICC divided in **2 parts (volumes)**

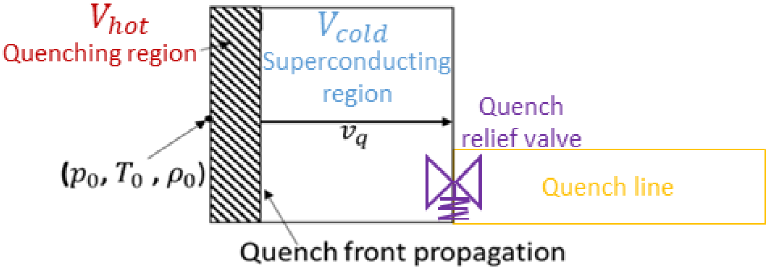

Energy balances:

$$P_J(t) = \frac{\eta_{Cu}\left(T_{cond}(t), RRR_{Cu}, B(t)\right)\,L_q(t)\,I(t)^2}{A_{Cu}}$$

$$\frac{dT_{cond}(t)}{dt} = \frac{P_{ext} + P_J(t) - h_{conv}\,P_{w,cond}\,L\,(T_{cond}(t) - T_{He}(t))}{L\,(A_{Cu}\,\rho_{Cu}\,C_{Cu}(t) + A_{NbTi}\,\rho_{NbTi}\,C_{NbTi}(t))}$$

$$\frac{dT_{He}(t)}{dt} = \frac{h_{conv}\,P_{w,cond}\left(T_{cond}(t) - T_{He}(t)\right) - h_{conv}\,P_{w,jacket}\left(T_{He}(t) - T_{jacket}(t)\right)}{A_{He}\,\rho_{He}(t)\,C_{He}(t)}$$

$$\frac{dT_{jacket}(t)}{dt} = \frac{h_{conv}\,P_{w,jacket}\left(T_{He}(t) - T_{jacket}(t)\right)}{A_{jacket}\,\rho_{jacket}\,C_{jacket}(t)}$$